

Estimate of $B(K \rightarrow \pi \nu \bar{\nu})|_{SM}$ from Standard Model fits to λ_t

S.H. Kettell,¹ L.G. Landsberg,² and H. Nguyen³

¹Brookhaven National Laboratory, Upton, New York USA

²Institute of High Energy Physics, Serpukhov, Russia

³Fermi National Accelerator Laboratory, Batavia, IL, USA

(Dated: October 31, 2018)

We estimate $B(K^+ \rightarrow \pi^+ \nu \bar{\nu})$ in the context of the Standard Model by fitting for $\lambda_t \equiv V_{td} V_{ts}^*$ of the ‘kaon unitarity triangle’ relation. We fit data from $|\varepsilon_K|$, the CP-violating parameter describing K -mixing, and $a_{\psi K}$, the CP-violating asymmetry in $B_d^0 \rightarrow J/\psi K^0$ decays. Our estimate is independent of the CKM matrix element V_{cb} and of the ratio of B-mixing frequencies $\Delta M_{B_s}/\Delta M_{B_d}$. The measured value of $B(K^+ \rightarrow \pi^+ \nu \bar{\nu})$ can be compared both to this estimate and to predictions made from $\Delta M_{B_s}/\Delta M_{B_d}$.

The ultra-rare FCNC kaon decays $K^+ \rightarrow \pi^+ \nu \bar{\nu}$ and $K_L^0 \rightarrow \pi^0 \nu \bar{\nu}$ are of particular interest as these ‘gold-plated decays’ can be predicted in the Standard Model framework with very high theoretical accuracy.

The $K \rightarrow \pi \nu \bar{\nu}$ decays are treated in detail in a number of papers[1–34]. We list some of the key aspects of these decays.

- The main contribution to these FCNC processes arises at small distances $r \sim 1/m_t, 1/m_Z$; therefore, a very accurate description for the strong interactions at the quark level is possible in the framework of perturbative QCD. This analysis has been carried out in the leading logarithmic order (LLO) with corrections to next to leading order (NLO)[1–4].
- The calculation of the matrix element $\langle \pi | H_w | K \rangle_{\pi \nu \bar{\nu}}$ from quark-level processes involves long-distance physics. However, these long-distance effects can be avoided by the renormalization procedure developed by Inami and Lim[5], relating the matrix element to that of the well known decay $K^+ \rightarrow \pi^0 e^+ \nu_e$ through isotopic-spin symmetry. Other possible long-distance contributions to $B(K^+ \rightarrow \pi^+ \nu \bar{\nu})$ have been shown to be negligible[6].
- Since the effective vertex $Z d \bar{s}$ in the diagrams of Figure 1 is short-distance, these processes are also sensitive to the contributions from new heavy objects (e.g., supersymmetric particles).

A very important step in the study of $K^+ \rightarrow \pi^+ \nu \bar{\nu}$ was achieved by the E787 experiment[7] at BNL in which two clean events were found in favorable background conditions, indicating a branching ratio of $B(K^+ \rightarrow \pi^+ \nu \bar{\nu}) = (15.7^{+17.5}_{-8.2}) \times 10^{-11}$. This observation has opened the door for future more precise study of the $K^+ \rightarrow \pi^+ \nu \bar{\nu}$ decay[8, 9].

In the Standard Model, the $K^+ \rightarrow \pi^+ \nu \bar{\nu}$ decay is described by penguin and box diagrams presented in Figure 1. The partial widths have the form:

$$\begin{aligned} \Gamma(K^+ \rightarrow \pi^+ \nu \bar{\nu}) &= \kappa^+ \cdot |\lambda_c F(x_c) + \lambda_t X(x_t)|^2 \\ &= \kappa^+ \cdot [(Re \lambda_c F(x_c) + Re \lambda_t X(x_t))^2 \\ &\quad + (Im \lambda_c F(x_c) + Im \lambda_t X(x_t))^2] \end{aligned}$$

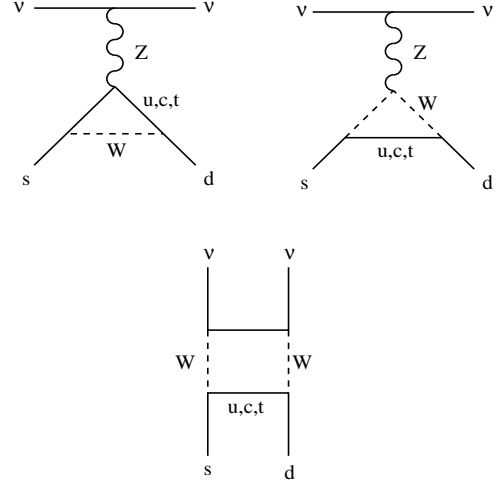


Figure 1: The dominant contributions to $K \rightarrow \pi \nu \bar{\nu}$.

$$\begin{aligned} &+ (Im \lambda_c F(x_c) + Im \lambda_t X(x_t))^2] \\ &\simeq \kappa^+ \cdot [(Re \lambda_c F(x_c) + Re \lambda_t X(x_t))^2 \\ &+ (Im \lambda_c F(x_c) + Im \lambda_t X(x_t))^2] \end{aligned} \quad (1)$$

where

$$\kappa^+ = \left(\frac{G_F}{\sqrt{2}} \right)^2 \cdot |\langle \pi^+ \nu \bar{\nu} | H_w | K^+ \rangle|^2 \cdot 3 \left(\frac{\alpha}{2\pi \sin^2 \vartheta_w} \right)^2$$

The factor of 3 in the expression for κ^+ results from the three flavors of neutrinos (ν_e, ν_μ, ν_τ) participating in the $K^+ \rightarrow \pi^+ \nu \bar{\nu}$ decays. The factors $F(x_c)$ and $X(x_t)$ are functions corresponding to the quark loops. These functions include the Inami-Lim functions[5] and the QCD corrections that have been calculated to NLO[1–4, 10]. They depend on the variables $x_i = (m_i/m_W)^2$ with the masses of the $+\frac{2}{3}$ quarks, $m_i : i = c, t$. The $\lambda_i \equiv V_{id} V_{is}^*$ are vectors in the complex plane that satisfy the unitarity relation:

$$\lambda_t + \lambda_c + \lambda_u = 0 \quad (\lambda_i = V_{id} V_{is}^* ; i = u, c, t). \quad (2)$$

This equation describes the ‘kaon unitarity triangle’, which can be completely determined from measurement of the three kaon decays: $K^+ \rightarrow \pi^0 e^+ \nu_e$, $K^+ \rightarrow \pi^+ \nu \bar{\nu}$ and

$K_L^0 \rightarrow \pi^0 \nu \bar{\nu}$. This triangle is highly elongated with a base to height ratio of ~ 1000 .

Using the values of m_c and m_t in Table I, the calculations from Reference 1 yield $F(x_c) = (9.8 \pm 1.8) \times 10^{-4}$ and $X(x_t) = (1.52 \pm 0.05)$. The accuracy improves with increasing quark mass, and there are systematic dependences on $\Lambda_{\overline{MS}}^{(4)}$. The c -quark contribution in (1) is smaller than the t -quark contribution, but is non-negligible. Although $F(x_c)/X(x_t) \sim 10^{-3}$, $Re\lambda_c$ is much larger than $Re\lambda_t$ and $Im\lambda_t$. ($Re\lambda_c \sim \lambda$ while $Re\lambda_t$, $Im\lambda_t$ and $Im\lambda_c$ are less than λ^5).

For the CP -violating[11, 12] $K_L^0 \rightarrow \pi^0 \nu \bar{\nu}$ decay

$$\begin{aligned} \Gamma(K_L^0 \rightarrow \pi^0 \nu \bar{\nu}) &\simeq \frac{1}{2} |A(K^0 \rightarrow \pi^0 \nu \bar{\nu}) - A(\bar{K}^0 \rightarrow \pi^0 \nu \bar{\nu})|^2 \\ &= \kappa^0 \cdot \frac{1}{2} |\lambda_c F(x_c) + \lambda_t X(x_t) - h.c.|^2 \\ &= \kappa^0 \cdot 2 [Im\lambda_c F(x_c) + Im\lambda_t X(x_t)]^2 \\ &\simeq \kappa^0 \cdot 2 [Im\lambda_t X(x_t)]^2 \end{aligned} \quad (3)$$

where

$$\kappa^0 = \left(\frac{G_F}{\sqrt{2}} \right)^2 \cdot |\langle \pi^0 \nu \bar{\nu} | H_w | K^0 \rangle|^2 \cdot 3 \left(\frac{\alpha}{2\pi \sin^2 \vartheta_w} \right)^2$$

The c -quark contribution is negligible since $Im\lambda_c F(x_c) \ll Im\lambda_t X(x_t)$.

The partial width for the well-known decay mode $K^+ \rightarrow \pi^0 e^+ \nu_e$ is given by:

$$\Gamma(K^+ \rightarrow \pi^0 e^+ \nu_e) = \left(\frac{G_F}{\sqrt{2}} \right)^2 |V_{us}|^2 |\langle \pi^0 e^+ \nu_e | H_w | K^+ \rangle|^2$$

As mentioned above, one can relate this to $\langle \pi^+ \nu \bar{\nu} | H_w | K^+ \rangle$ and $\langle \pi^0 \nu \bar{\nu} | H_w | K^0 \rangle$ with the help of isotopic-spin symmetry:

$$\left| \frac{\langle \pi^+ \nu \bar{\nu} | H_w | K^+ \rangle}{\langle \pi^0 e^+ \nu_e | H_w | K^+ \rangle} \right|^2 = \left| \frac{\langle \pi^+ | H_w | K^+ \rangle}{\langle \pi^0 | H_w | K^+ \rangle} \right|^2 = 2r_+, \quad (4)$$

$$\left| \frac{\langle \pi^0 \nu \bar{\nu} | H_w | K^0 \rangle}{\langle \pi^0 e^+ \nu_e | H_w | K^+ \rangle} \right|^2 = \left| \frac{\langle \pi^0 | H_w | K^0 \rangle}{\langle \pi^0 | H_w | K^+ \rangle} \right|^2 = r_0. \quad (5)$$

The factor 2 in (4) accounts for the pion quark structure $|\pi^0\rangle = \frac{1}{\sqrt{2}}|u\bar{u} - d\bar{d}\rangle$ and $|\pi^+\rangle = |u\bar{d}\rangle$. The factors $r_+ = 0.901$ and $r_0 = 0.944$ arise from the phase space corrections and the breaking of isotopic symmetry[13].

Hence from (1), (4) and (5) the branching ratio for the $K^+ \rightarrow \pi^+ \nu \bar{\nu}$ decay is

$$\begin{aligned} B(K^+ \rightarrow \pi^+ \nu \bar{\nu})|_{SM} &= R_+ \cdot \frac{X(x_t)^2}{\lambda^2} \\ &\cdot \left\{ [Re\lambda_c f \frac{F(x_c)}{X(x_t)} + Re\lambda_t]^2 + [Im\lambda_t]^2 \right\} \end{aligned} \quad (6)$$

where

$$\left. \begin{aligned} R_+ &= B(K^+ \rightarrow \pi^0 e^+ \nu_e) \cdot \frac{3\alpha^2}{2\pi^2 \sin^4 \vartheta_w} \cdot r_+ \\ &= 7.50 \times 10^{-6} \\ f \frac{F(x_c)}{X(x_t)} &= (6.66 \pm 1.23) \times 10^{-4} \\ f &= 1.03 \pm 0.02 \end{aligned} \right\} \quad (7)$$

Here, f is an additional correction factor to the c -quark term to take into account non-perturbative effects of dimension-8 operators[14]. The branching ratio for the $K_L^0 \rightarrow \pi^0 \nu \bar{\nu}$ decay is

$$B(K_L^0 \rightarrow \pi^0 \nu \bar{\nu})|_{SM} = R_0 \cdot \frac{X(x_t)^2}{\lambda^2} [Im\lambda_t]^2 \quad (8)$$

with

$$\begin{aligned} R_0 &= R_+ \cdot \frac{r_0}{r_+} \cdot \frac{\tau(K_L^0)}{\tau(K^+)} = 3.28 \times 10^{-5} \\ r_0/r_+ &= 1.048 \quad \tau(K_L^0)/\tau(K^+) = 4.17 \end{aligned}$$

The intrinsic theoretical uncertainty of the SM prediction for $B(K^+ \rightarrow \pi^+ \nu \bar{\nu})|_{SM}$ is $\sim 7\%$ and is limited by the c -quark contribution, whereas for $B(K_L^0 \rightarrow \pi^0 \nu \bar{\nu})|_{SM}$ the uncertainty is 1–2%. However, in practice the uncertainties of the numerical evaluations of the $K \rightarrow \pi \nu \bar{\nu}$ branching ratios are dominated by the current uncertainties in the CKM matrix parameters.

The parameters $Im\lambda_t$, $Re\lambda_t$, $Re\lambda_c$ can be estimated within the standard unitarity triangle (UT) framework using the improved Wolfenstein parameterization[15] $\bar{\eta}$, $\bar{\rho}$, A , and λ (with $A\lambda^2 = |V_{cb}|$, $\bar{\rho} \equiv \rho(1 - \frac{\lambda^2}{2})$ and $\bar{\eta} \equiv \eta(1 - \frac{\lambda^2}{2})$). To $O(\lambda^4)$ the CKM matrix is

$$\begin{aligned} V_{CKM} &= \begin{pmatrix} V_{ud} & V_{us} & V_{ub} \\ V_{cd} & V_{cs} & V_{cb} \\ V_{td} & V_{ts} & V_{tb} \end{pmatrix} \\ &= \begin{pmatrix} 1 - \frac{\lambda^2}{2} & \lambda & A\lambda^3(\rho - i\eta) \\ -\lambda & 1 - \frac{\lambda^2}{2} & A\lambda^2 \\ A\lambda^3(1 - \rho - i\eta) & -A\lambda^2 & 1 \end{pmatrix} \\ &+ O(\lambda^4) \end{aligned} \quad (9)$$

and to higher order we have

$$\left. \begin{aligned} Re\lambda_c &= -\lambda \left(1 - \frac{\lambda^2}{2} \right) + O(\lambda^5) \\ Re\lambda_t &= -A^2 \lambda^5 \left(1 - \frac{\lambda^2}{2} \right) (1 - \bar{\rho}) + O(\lambda^7) \\ Im\lambda_t &= \eta A^2 \lambda^5 + O(\lambda^9) \end{aligned} \right\} \quad (10)$$

The current values of these and other parameters used in this paper can be found in Table I. Using (10) and Reference 35 (see Table I), equations (6) and (8) can be naively solved to give the branching ratios for $K^+ \rightarrow \pi^+ \nu \bar{\nu}$ and $K_L^0 \rightarrow \pi^0 \nu \bar{\nu}$:

$$\begin{aligned}
B(K^+ \rightarrow \pi^+ \nu \bar{\nu})|_{SM} &= R_+ \cdot A^4 \lambda^8 X(x_t)^2 \cdot \left\{ \frac{1}{\sigma} [(\rho_0 - \bar{\rho})^2 + (\sigma \bar{\eta})^2] \right\} \\
&= R_+ \cdot |V_{cb}|^4 X(x_t)^2 \cdot \left\{ \frac{1}{\sigma} [(\rho_0 - \bar{\rho})^2 + (\sigma \bar{\eta})^2] \right\} \\
&= 7.50 \times 10^{-6} \cdot [2.88 \times 10^{-6} \pm (19.4\%)] [2.30 \pm (6.9\%)] \{1.44 \pm (20\%)\} \\
&= [7.15 \pm (28.9\%)] \times 10^{-11} = [7.2 \pm 2.1] \times 10^{-11}
\end{aligned} \tag{11}$$

$$\begin{aligned}
B(K_L^0 \rightarrow \pi^0 \nu \bar{\nu})|_{SM} &= R_0 \cdot A^2 \lambda^8 X(x_t)^2 \cdot \{\sigma \bar{\eta}^2\} \\
&= R_0 \cdot |V_{cb}|^4 X(x_t)^2 \cdot \{\sigma \bar{\eta}^2\} \\
&= 3.28 \times 10^{-5} \cdot [2.88 \times 10^{-6} \pm (19.4\%)] [2.30 \pm (6.9\%)] \cdot \{0.129 \pm (28.6\%)\} \\
&= [2.8 \pm (35\%)] \times 10^{-11} = [2.8 \pm 1.0] \times 10^{-11}
\end{aligned} \tag{12}$$

with $\rho_0 = 1 + \Delta = 1 + fF(x_c)/(|V_{cb}|^2 X(x_t)) = 1.40 \pm 0.08$ and $\sigma = 1/(1 - \frac{1}{2}\lambda^2)^2 = 1.051$.

The uncertainties of $B(K \rightarrow \pi \nu \bar{\nu})$ in (11) and (12) are dominated by the current uncertainties in the CKM parameters and are significantly larger than the intrinsic theoretical uncertainties. The uncertainty of $|V_{cb}|$ is quite significant in the evaluation of $B(K \rightarrow \pi \nu \bar{\nu})$ due to the $|V_{cb}|^4$ dependence. CLEO has recently measured[36] a somewhat higher $|V_{cb}|$ value of $(46.9 \pm 3.0) \times 10^{-3}$, which would cause a significant increase to $B(K \rightarrow \pi \nu \bar{\nu})$ in equations (11) and (12).

The numerical solutions of equations (11) and (12) do not include correlations between $\bar{\rho}$, $\bar{\eta}$, X and V_{cb} . Rather, these calculation are used to demonstrate the influence of different factors in the calculation of $B(K \rightarrow \pi \nu \bar{\nu})$. An evaluation[16] employing a scanning method and conservative errors for V_{CKM} obtained the following values: $B(K^+ \rightarrow \pi^+ \nu \bar{\nu})|_{SM} = (7.5 \pm 2.9) \times 10^{-11}$ and $B(K_L^0 \rightarrow \pi^0 \nu \bar{\nu})|_{SM} = (2.6 \pm 1.2) \times 10^{-11}$. A more recent evaluation with similar CKM inputs, but employing a Gaussian fit obtained $B(K^+ \rightarrow \pi^+ \nu \bar{\nu})|_{SM} = (7.2 \pm 2.1) \times 10^{-11}$ [17]. These values are not very different from the results in equations (11) and (12). In some recent analyses[18–21] with correlations included higher precision on $B(K \rightarrow \pi \nu \bar{\nu})$ has been obtained.

For the values of the parameters $|V_{cb}|$, $\bar{\rho}$ and $\bar{\eta}$ in equations (11) and (12) we adopt the more conservative approach of Reference 35. A more aggressive approach[22] for the evaluation of these errors can significantly increase the precision for $B(K \rightarrow \pi \nu \bar{\nu})$. Solving equations (11) and (12) with these values gives $B(K^+ \rightarrow \pi^+ \nu \bar{\nu})|_{SM} = (7.4 \pm 1.2) \times 10^{-11}$ and $B(K_L^0 \rightarrow \pi^0 \nu \bar{\nu})|_{SM} = (2.8 \pm 0.5) \times 10^{-11}$. The precision of the outputs of the standard UT fits is dependent on the value of ξ , the SU(3) breaking correction to $\Delta M_{B_s}/\Delta M_{B_d}$. The generally accepted value of ξ is $\xi = 1.15 \pm 0.06$; however, recent work would suggest a higher value of $\xi = 1.18 \pm 0.04_{-0.0}^{+0.12}$ [37] (or even as high as $\xi = 1.32 \pm 0.10$ [38].)

Given the strong dependence of equations (11) and (12) on $|V_{cb}|$, we consider an estimate of $B(K^+ \rightarrow \pi^+ \nu \bar{\nu})$ that is essentially independent of $|V_{cb}|$. This estimate is also independent of $\Delta M_{B_s}/\Delta M_{B_d}$. It is based solely on $|\varepsilon_K|$ and $a_{\psi K}$, is remarkably competitive to other estimates, and has the advantage of simplicity.

In this work we directly evaluate λ_t to calculate $B(K \rightarrow \pi \nu \bar{\nu})$ from (6) and (8). This avoids the use of $\bar{\rho}$ and $\bar{\eta}$, as has been used in previous calculations of $B(K \rightarrow \pi \nu \bar{\nu})$. This approach has been discussed in the literature[23, 24], but as far as we know, no calculations of $B(K \rightarrow \pi \nu \bar{\nu})$ exist by this method. In order to minimize uncertainty from $|V_{cb}|$, it is natural to consider $|\varepsilon_K|$ and $a_{\psi K}$ in terms of the kaon UT¹. We recall that $\lambda_u = V_{ud}V_{us}^* \simeq \lambda(1 - \frac{1}{2}\lambda^2)$ is real, and $\lambda_c = V_{cd}V_{cs}^*$ has a very small complex phase $\varphi(\lambda_c) \simeq \text{Im}\lambda_t/\lambda \simeq 6 \times 10^{-4}$. The phase of V_{ts} is $\varphi(V_{ts}) \simeq -\pi + \text{Im}\lambda_t * \lambda/|V_{cb}|^2 = -\pi + 0.0172 = -\pi + 1.0^\circ$. The phase of V_{td} is $\varphi(V_{td}) = -\beta$ and the angle (β_K) between λ_t and λ_u is

$$\begin{aligned}
\beta_K &= \pi - \varphi(V_{td}V_{ts}^*) = \pi - \varphi(V_{td}) + \varphi(V_{ts}) = \beta + 1.0^\circ \\
&= (24.6 \pm 2.3)^\circ
\end{aligned} \tag{13}$$

This angle is very close to β , which in the SM is extracted cleanly from the precise measurement of $a_{\psi K}$, the CP asymmetry in $B_d^0 \rightarrow J/\psi K^0$ decays: $\sin 2\beta = 0.734 \pm 0.054$ [39]. We use an iterative procedure, starting with $\beta_K = \beta$, from our fit to derive $\text{Im}\lambda_t$ and recalculate $\beta_K = \beta + \text{Im}\lambda_t * \lambda/|V_{cb}|^2$. This procedure converges after one iteration since the correction to β is small. There is also a small dependence on $|V_{cb}|$; however, a 10% change in

¹ We expect that a precise determination of the apex of the kaon UT (λ_t^a) will be available, entirely from kaon decay data, in the near future. In the meantime, it is necessary to use some data from the B-system, so we chose to augment $|\varepsilon_K|$ with the theoretically clean measurement of the CP asymmetry $a_{\psi K}$ from the B-system.

$|V_{cb}|$ results in only a 0.6% shift in $B(K^+ \rightarrow \pi^+ \nu \bar{\nu})$, which is significantly less than the uncertainty in our result. For all practical purposes our result is independent of $|V_{cb}|$. The preferred solution for β , based on other SM input, such as V_{ub}/V_{cb} is $\beta = (23.6 \pm 2.3)^\circ$, so we shall only consider this particular solution. The extraction of $\sin 2\beta$ from $a_{\psi K}$ is also clean in models with Minimal Flavor Violation (MFV)[22, 25, 26]. In these models there are no new phases and all of the influences of new physics are in modifications to the Inami-Lim functions.

In the Standard Model, the apex of the kaon UT (λ_t^a) is constrained by various measurements as shown in Figure 2 (without errors). The constraint from $|\varepsilon_K|$ is expressed as [10, 40–42]

$$|\varepsilon_K| = L \cdot \hat{B}_K \text{Im} \lambda_t \cdot \{ \text{Re} \lambda_c [\eta_{cc} S_0(x_c) - \eta_{ct} S_0(x_c; x_t)] - \text{Re} \lambda_t \cdot \eta_{tt} \cdot S_0(x_t) \} \quad (14)$$

with parameters as shown in Table I. We can find the apex of the kaon UT as the intercept of the $|\varepsilon_K|$ curve with the line representing the constraint from $a_{\psi K}$:

$$\text{Im} \lambda_t = -\tan \beta_K \cdot \text{Re} \lambda_t = (-0.458 \pm 0.049) \cdot \text{Re} \lambda_t \quad (15)$$

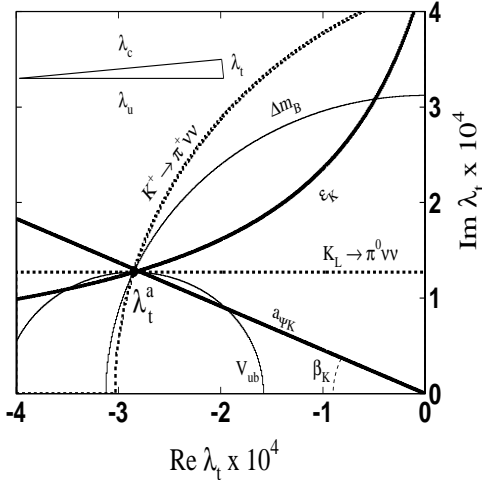


Figure 2: The apex of the kaon unitarity triangle is λ_t^a (no errors are shown). The circle labeled V_{ub} is described by (24) with a radius $R \sim V_{cb} V_{ub}$. The thick black lines ($|\varepsilon_K|$ and $a_{\psi K}$) illustrate the main constraints used in this paper. The dashed lines illustrate the constraints from $K \rightarrow \pi \nu \bar{\nu}$. The constraint from ΔM_{B_d} is shown as the circle centered at the origin. The inset shows the triangle (not drawn to scale).

To calculate a probability density function (PDF) for λ_t^a , we follow the Bayesian approach of References 43, 44, and 22. Let $f(\mathbf{x})$ be the PDF for \mathbf{x} , where \mathbf{x} is a point in the space of $(\beta_K, |\varepsilon_K|, \hat{B}_K, m_t, m_c, \lambda, \alpha_s, \eta_{cc}, \eta_{ct}, \eta_{tt})$. Equations (14) and (15) define the mapping from \mathbf{x} to λ_t^a . Through these equations and $f(\mathbf{x})$, we derive $f(\lambda_t^a)$, the PDF for λ_t^a . $f(\mathbf{x})$ depends on the PDF's for the components of \mathbf{x} . We assume that the component PDF's are independent from one another except for the small dependence

of η_{cc} on m_c and α_s (discussed below). The component PDF's are taken from Table I.

Figure 3 shows the PDF for λ_t^a . We find the following central values:

$$\left. \begin{aligned} \text{Re} \lambda_t^a &= (-2.85 \pm 0.29) \times 10^{-4} \\ \text{Im} \lambda_t^a &= (1.30 \pm 0.12) \times 10^{-4} \end{aligned} \right\} \quad (16)$$

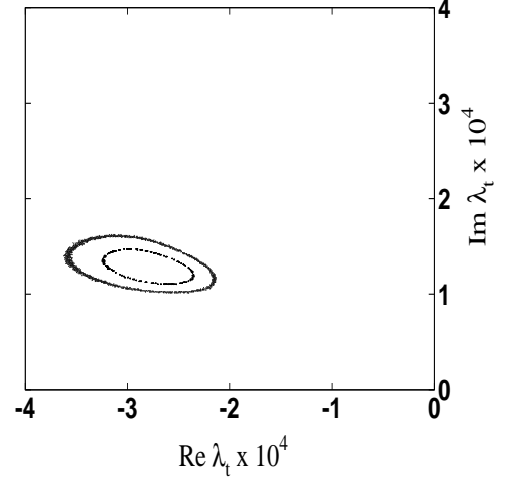


Figure 3: 1 σ and 2 σ C.L. intervals on λ_t^a , obtained from the measurements of $|\varepsilon_K|$ and $a_{\psi K}$.

For $B(K^+ \rightarrow \pi^+ \nu \bar{\nu})|_{SM}$ we obtain from Equations (6) and (16):

$$\begin{aligned} B(K^+ \rightarrow \pi^+ \nu \bar{\nu})|_{SM} &= \left\{ [\text{Re} \lambda_c f F(x_c) + X(x_t) \text{Re} \lambda_t^a]^2 \right. \\ &\quad \left. + [X(x_t) \text{Im} \lambda_t^a]^2 \right\} \cdot \frac{R_+}{\lambda^2} \\ &= (7.07 \pm 1.03) \times 10^{-11} \end{aligned} \quad (17)$$

The three largest contributions to the uncertainty are due to \hat{B}_K (0.69×10^{-11}), m_c (0.44×10^{-11}) and $a_{\psi K}$ (0.49×10^{-11}). The probability distribution for $B(K^+ \rightarrow \pi^+ \nu \bar{\nu})|_{SM}$ is presented in Figure 4.

In obtaining the results of equation (17) we have accounted for the correlations between $|\varepsilon_K|$ (one of the inputs for determining λ_t^a), $F(x_c)$ and $X(x_t)$ through the variables x_c , x_t , and $\Lambda_{MS}^{(4)}$. The functions $X(x_t)$ and $F(x_c, \Lambda_{MS}^{(4)})$ are given in Reference 1, from which we have parameterized Table 1 to get:

$$\begin{aligned} F(x_c, \Lambda_{MS}^{(4)}) \times 10^4 &= 9.82 + 16.58(m_c - 1.3) \\ &\quad + 7.8(0.325 - \Lambda_{MS}^{(4)}) \end{aligned} \quad (18)$$

where

$$\Lambda_{MS}^{(4)} [GeV] = 0.341 + 16.7(-0.119 + \alpha_s(M_Z)) \quad (19)$$

Equation (19) is accurate to 0.7% for α_s in the range 0.116 to 0.122[45]. The expression for $|\varepsilon_K|$ (and the determination of the apex, λ_t^a) has a dependence on x_c and

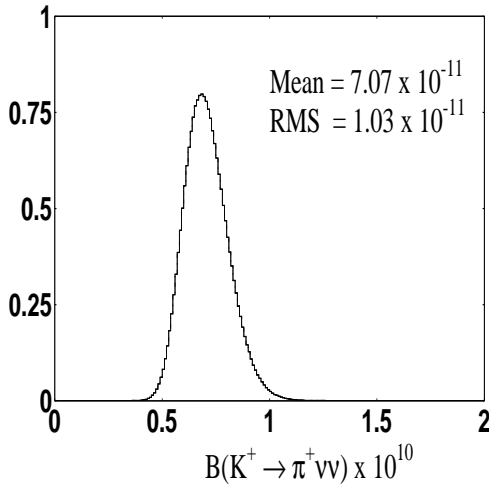


Figure 4: The PDF for $B(K^+ \rightarrow \pi^+ \nu \bar{\nu})|_{SM}$, obtained from the measurements of $|\varepsilon_K|$ and $a_{\psi K}$. The 95% C.L. upper limit is 8.9×10^{-11} and 95% C.L. lower limit is 5.6×10^{-11} .

x_t through the Inami-Lim functions $S_0(x_c)$, $S_0(x_t)$ and $S_0(x_c, x_t)$. In addition, the NLO correction η_{cc} has the following dependence[45]:

$$\eta_{cc} = (1.46 \pm \sigma_1)(1 - 1.2(\frac{m_c}{1.25} - 1)) \times (1 + 52(\alpha_s(M_Z) - 0.118)) \quad (20)$$

with

$$\sigma_1 = 0.31(1 - 1.8(\frac{m_c}{1.25} - 1))(1 + 80(\alpha_s(M_Z) - 0.118)) \quad (21)$$

The largest correlation through m_c causes both endpoints of the vector describing $B(K^+ \rightarrow \pi^+ \nu \bar{\nu})$, λ_t^a and $\frac{Re\lambda_c f_F(x_c)}{X(x_t)}$ to move in similar directions, so that the uncertainty on the length of the vector is smaller than the uncertainties in either endpoint. Inclusion of the correlations due to x_c , x_t and $\Lambda_{MS}^{(4)}$ reduces the uncertainty in $B(K^+ \rightarrow \pi^+ \nu \bar{\nu})|_{SM}$ by $\sim 20\%$.

For $K_L^\circ \rightarrow \pi^\circ \nu \bar{\nu}$ we obtain from (8) and (16):

$$B(K_L^\circ \rightarrow \pi^\circ \nu \bar{\nu})|_{SM} = R_0 \frac{X(x_t)^2}{\lambda^2} [Im\lambda_t^a]^2 = (2.60 \pm 0.52) \times 10^{-11} \quad (22)$$

The four largest contributions to the uncertainty are due to \hat{B}_K (0.37×10^{-11}), $a_{\psi K}$ (0.23×10^{-11}), m_c (0.16×10^{-11}) and m_t (0.08×10^{-11}).

The results of these new calculations (17) and (22) of $K \rightarrow \pi \nu \bar{\nu}$ branching ratios from fits to λ_t are in a good agreement with the calculations based on the standard unitarity triangle variables (11) and (12) but are free of uncertainties in $|V_{cb}|$ and are independent of $\Delta M_{B_s}/\Delta M_{B_d}$. The main source of uncertainty in (17) and (22) is the lattice calculation of $\hat{B}_K = 0.86 \pm 0.15$. (We note that some lattice calculations using domain-wall fermions[18, 46, 47]

find values of \hat{B}_K that are 10–15% lower than the recent world average[37, 48] that we use in Table I.) If future lattice QCD calculations[49] can significantly reduce the uncertainty in \hat{B}_K , an improvement in $B(K \rightarrow \pi \nu \bar{\nu})|_{SM}$ will be possible.

Given the difficulty of assigning PDF's to theoretical uncertainties, we explore the influence of a more conservative scanning technique on the uncertainty in $B(K^+ \rightarrow \pi^+ \nu \bar{\nu})|_{SM}$. We determine λ_t^a again from only $|\varepsilon_K|$ and $a_{\psi K}$, using gaussian errors for all quantities except \hat{B}_K and m_c , which are scanned throughout their ranges: $0.72 < \hat{B}_K < 1.0$ and $1.2 < m_c < 1.4$. For $\hat{B}_K = 0.72$ and $m_c = 1.4$, which maximizes $B(K^+ \rightarrow \pi^+ \nu \bar{\nu})$, the 95% CL upper limit is $B(K^+ \rightarrow \pi^+ \nu \bar{\nu})|_{SM} < 9.9 \times 10^{-11}$. For $\hat{B}_K = 1.00$ and $m_c = 1.2$, which minimizes $B(K^+ \rightarrow \pi^+ \nu \bar{\nu})$, the 95% CL lower limit is $B(K^+ \rightarrow \pi^+ \nu \bar{\nu})|_{SM} > 5.0 \times 10^{-11}$. These limits are not much worse than those derived from Figure 4.

We've emphasized that our estimate uses only $a_{\psi K}$ and $|\varepsilon_K|$. Nevertheless, it is interesting to consider how the measurements of ΔM_{B_d} and $|V_{ub}|$ would constrain λ_t^a . Here we will use the more aggressive treatment of $|V_{cb}|$ errors (see Table I) in order to obtain the smallest errors on $B(K^+ \rightarrow \pi^+ \nu \bar{\nu})$. From the following relations:

$$\Delta m_{B_d} = \frac{G_F}{6\pi^2} M_W^2 m_{B_d} f_{B_d}^2 \hat{B}_{B_d} \eta_{B_d} S_0(x_t) |V_{td} V_{tb}^*|^2$$

$$0 = V_{ud} V_{ub}^* + V_{cd} V_{cb}^* + V_{td} V_{tb}^*$$

and using the approximations of (9): $V_{tb}^* \approx 1$, $V_{us} = \lambda$, $V_{ud} \approx (1 - \lambda^2/2)$, and $V_{cb} \approx -V_{ts}$, we convert the equations above into:

$$\Delta m_{B_d} = \frac{G_F}{6\pi^2} M_W^2 m_{B_d} f_{B_d}^2 \hat{B}_{B_d} \eta_{B_d} S_0(x_t) \frac{|\lambda_t|^2}{|V_{cb}|^2} \quad (23)$$

$$|\lambda_t| = |V_{ub}^* V_{cb}^* (1 - \lambda^2/2) - \lambda (V_{cb}^*)^2| \quad (24)$$

These two equations describe two circles whose intersections contain the apex of the kaon UT (see Fig. 2), and are correlated somewhat through V_{cb} . Similar to the case of $|\varepsilon_K|$, with large uncertainties from \hat{B}_K , there are large uncertainties in the extraction of λ_t^a from the ΔM_{B_d} and $|V_{ub}|$ constraints, with large uncertainties from $f_{B_d}^2 \hat{B}_{B_d}$, $|V_{ub}|$ and $|V_{cb}|$. The uncertainty on the constraint from B-mixing may be significantly improved by the addition of ΔM_{B_s} , once the situation with ξ is resolved (this will be further improved once ΔM_{B_s} is actually observed). Using the Bayesian procedure described earlier and the parameters in Table I, the PDF for λ_t^a derived solely from the constraints of ΔM_{B_d} and $|V_{ub}|$ is shown in Fig. 5. We see that this PDF does not constrain the kaon UT apex as well as $a_{\psi K}$ and $|\varepsilon_K|$. Combining all four constraints, we get the PDF for $B(K^+ \rightarrow \pi^+ \nu \bar{\nu})$ shown in Fig. 6, which is only slightly more precise than Fig. 4. From this combined

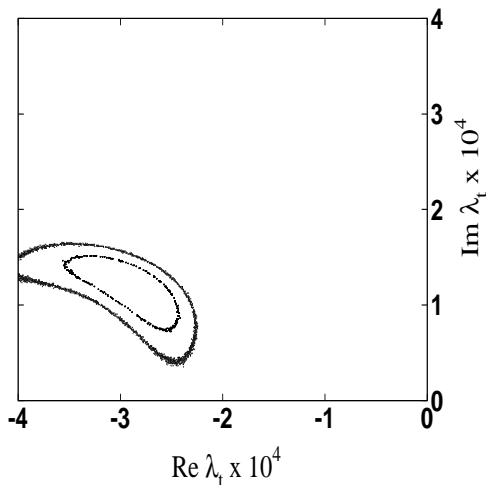


Figure 5: 1σ and 2σ C.L. intervals on λ_t^a , obtained from the constraints of ΔM_{B_d} and $|V_{ub}|$.

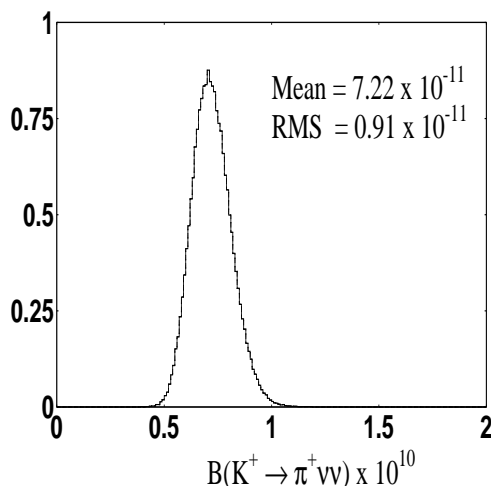


Figure 6: The PDF for $B(K^+ \rightarrow \pi^+ \nu \bar{\nu})|_{SM}$ obtained from the constraints from $|\varepsilon_K|$, $a_{\psi K}$, ΔM_{B_d} , and $|V_{ub}|$.

analysis we obtain

$$\begin{aligned} B(K^+ \rightarrow \pi^+ \nu \bar{\nu})|_{SM} &= (7.22 \pm 0.91) \times 10^{-11} \\ B(K_L^0 \rightarrow \pi^0 \nu \bar{\nu})|_{SM} &= (2.49 \pm 0.42) \times 10^{-11}. \end{aligned} \quad (25)$$

The CKM matrix appears to be the dominant source of CP violation. However, some models[50] allow for a significant contribution of new physics to $B(K \rightarrow \pi \nu \bar{\nu})$ while preserving the equality between $\sin 2\beta$ as measured from $a_{\psi K}$ and global CKM fits. A crucial test of the CKM description will be to compare β derived from $B(K \rightarrow \pi \nu \bar{\nu})$ to that from $a_{\psi K}$ [12, 27–29]. The most important new information on the CKM matrix will be measurements of $B(K^+ \rightarrow \pi^+ \nu \bar{\nu})$ [9] and $B(K_L^0 \rightarrow \pi^0 \nu \bar{\nu})$ [51] to 10% precision. The combination of these, in context of the SM, will determine $\sin 2\beta$ to 0.05[30], competitive with the current uncertainty on $\sin 2\beta$. The comparison of this angle obtained from $B(K \rightarrow \pi \nu \bar{\nu})$ with that from $a_{\psi K}$ will provide

a very strong test of the SM description of CP-violation.

Another critical test of the SM will be the direct comparison of $B(K^+ \rightarrow \pi^+ \nu \bar{\nu})$ to either $\Delta M_{B_s}/\Delta M_{B_d}$, which in the SM both directly measure $|V_{td}|$, or to evaluations of $B(K^+ \rightarrow \pi^+ \nu \bar{\nu})|_{SM}$ such as this work. Currently, the E787 measurement of $B(K^+ \rightarrow \pi^+ \nu \bar{\nu}) = (15.7_{-8.2}^{+17.5}) \times 10^{-11}$ is consistent with the SM expectation, but the central experimental value exceeds it by a factor of two. To date there is only a limit on $\Delta M_{B_s} > 14.4 ps^{-1}$ (95% C.L.)[52], but it is likely to be observed soon. Until ΔM_{B_s} is observed, this limit can be used to set an upper limit on $B(K^+ \rightarrow \pi^+ \nu \bar{\nu})$ [1]. A recent calculation of this limit[17] gives $B(K^+ \rightarrow \pi^+ \nu \bar{\nu})|_{SM} < 13.2 \times 10^{-11}$, which is below the central experimental value[7]. This work used a value of $\xi = 1.15 \pm 0.06$, whereas a higher value of ξ would raise this upper limit. Our work is an estimation of $B(K^+ \rightarrow \pi^+ \nu \bar{\nu})|_{SM}$ based solely on $|\varepsilon_K|$ and $a_{\psi K}$ and is not dependent on $|V_{cb}|$ or $\Delta M_{B_s}/\Delta M_{B_d}$. Our 95% C.L. upper limit is 8.9×10^{-11} with the largest systematic error of this approach coming from \hat{B}_K . The uncertainty from our prediction is comparable to the expected experimental uncertainties that might be achieved in the future measurements of $K^+ \rightarrow \pi^+ \nu \bar{\nu}$ [8, 9]. An experimental measurement significantly larger than determined from $\Delta M_{B_s}/\Delta M_{B_d}$ or our 99% C.L. limit of $B(K^+ \rightarrow \pi^+ \nu \bar{\nu})|_{SM} < 10 \times 10^{-11}$ will be a strong indication of new physics.

ACKNOWLEDGMENTS

We would like to thank P. Cooper, G. Isidori, D.E. Jaffe, P. Mackenzie, U. Nierste, L. Okun and A. Soni for useful discussions and comments and W. Marciano for the original stimulation to perform this type of calculation. This work was in part supported by the U.S. Department of Energy through contract #DE-AC02-98CH10886, in part by the Fermilab Particle Physics Division and in part by IHEP. L.G.L. is grateful to the Fermilab Administration and Particle Physics Division for their hospitality and support for his stay at Fermilab during the preparation of this work.

NOTE

During the final preparation of this work for publication we found that Reference 56 considered fitting for the apex of the UT from the CP-violating data only ($|\varepsilon_K|$ and $a_{\psi K}$), as we do. However, Reference 56 used $(\bar{\rho}, \bar{\eta})$, which is dependent on $|V_{cb}|$ and is not as suitable for analysis of $K \rightarrow \pi \nu \bar{\nu}$.

[1] G. Buchalla and A.J. Buras, Nucl. Phys. **B548**, 309 (1999) [hep-ph/9901288].

- [hep-ex/9909003]; B. Aubert *et al.* (BaBar), Phys. Rev. Lett. **89**, 201802 (2002) [hep-ex/0207042]; A. Abe *et al.* (Belle), Phys. Rev. **D66**, 071102 (2002) [hep-ex/0207098]. (see also J.L. Rosner, [hep-ph/0208243]).
- [40] S. Herrlich and U. Nierste, Nucl. Phys. **B419**, 292 (1994) [hep-ph/9310311].
- [41] S. Herrlich and U. Nierste, Phys. Rev. **D52** 6505 (1995) [hep-ph/9507262]; S. Herrlich and U. Nierste, Nucl. Phys. **B476** 27 (1996) [hep-ph/9604330].
- [42] A.J. Buras *et al.*, Nucl. Phys. **B347**, 491 (1990).
- [43] M. Ciuchini *et al.*, JHEP **0107**, 13 (2001) [hep-ph/0012308].
- [44] D.E. Jaffe and S. Youssef, Comp. Phys. Comm. **101**, 206 (1997) [hep-ph/9607469].
- [45] Ulrich Nierste private communication.
- [46] A. Ali Kahn *et al.* (CP-PACS) Phys. Rev. **D64**, 114506 (2001) [hep-lat/0105020].
- [47] T. Blum *et al.* (RBC) [hep-lat/0110075] (2001).
- [48] N. Garron *et al.*, [hep-lat/0212015].
- [49] P. Mackenzie, Talk on Fermilab Joint Experimental Theoretical Seminar, September 27, 2002.
- [50] J.A. Aguilar-Saavedra, Phys. Rev. **D67**, 035003 (2003) [hep-ph/0210112].
- [51] D.A. Bryman and L. Littenberg, Nucl. Phys. Proc. Suppl. **99B**, 61 (2001). <http://pubweb.bnl.gov/users/e926/www>
- [52] http://lepbose.web.cern.ch/LEPBOSC/combined_results/amsterdam_2002
- [53] Results presented at the CKM Unitary Triangle Workshop, CERN Feb. 2002. <http://ckm-workshop.web.cern.ch/ckm-workshop> [hep-ph/0304132]
- [54] M. Artuso and E. Barberio [hep-ph/0205163]
- [55] D. Becirevic *et al.*, [hep-ph/0211271].
- [56] A. Stocchi, [hep-ph/0211245].